Electronic Supplementary Material (ESI) for Physical Chemistry Chemical Physics.


# Supplementary Information For

# Unexpected Electrophiles in the Atmosphere, Anhydride Nucleophile Reactions and Uptake to Biomass Burning Emissions

Max Loebel Roson,[†] Maya Abou-Ghanem,[‡,†] Erica Kim,[†] Shuang Wu,[†] Dylan Long,[†] Sarah A. Styler,[¶,†] and Ran Zhao[*,†]

[†]*Department of Chemistry, University of Alberta, Edmonton, Alberta T6G 2G2, Canada*

[‡]*NOAA Chemical Sciences Laboratory, Boulder, United States of America*

[¶]*Department of Chemistry & Chemical Biology, Hamilton, L8S 4M1, Canada*

E-mail: rz@ualberta.ca

## Section S.I.1 $^1$H NMR Analysis

As shown in Figure S.I.2, maleic anhydride will hydrolyse in the protic solvent ($D_2O$), yielding a peak a ∼6.4 ppm. Both (Figures S.I.3 and S.I.4) also display the same peak, indicating it is due to maleic acid. The acid peak is not present in the aprotic solvent (Figure S.I.1) which instead displays a peak shift of ∼7.1 ppm due to the anhydride. As can be seen in Table S.I.1, the calculated concentration of maleic anhydride in $D_2O$ (obtained from the acid peak shift of ∼6.4 ppm) is similar to the concentration of the maleic acid standards. This indicates the anhydride fully hydrolyses into its acid form. The peak shifts of ∼4.7 and ∼7.4 ppm represent the solvents $D_2O$ and $CDCl_3$ respectively. All samples display a strong internal standard (DMSO) peak shift, at 2.62 ppm using $CDCl_3$ as a solvent, and 2.71 for $D_2O$, as predicted by established literature.[1] The calculated concentration is obtained from the anhydride or acid peak intensity compared to that of the of the internal standard.

Table S.I.1: $^1$H NMR anhydride and acid analysis in protic ($D_2O$) and aprotic ($CDCl_3$) solvents. The calculated concentration range represents duplicate analyses.

| Chemical | Solvent | DMSO (mM) | Calculated Conc. (mM) |
|---|---|---|---|
| Maleic Anhydride* | $D_2O$ | 0.5 | 0.00342 - 0.00362 |
| Maleic Anhydride | $CDCl_3$ | 0.5 | 0.00345 - 0.00367 |
| Maleic Acid | $D_2O$ | 0.5 | 0.00399 - 0.00407 |
| Maleic Acid | $CDCl_3$ | 0.5 | 0.00365 - 0.00408 |

*Lacking maleic anhydride peak, concentration calculated from maleic acid.

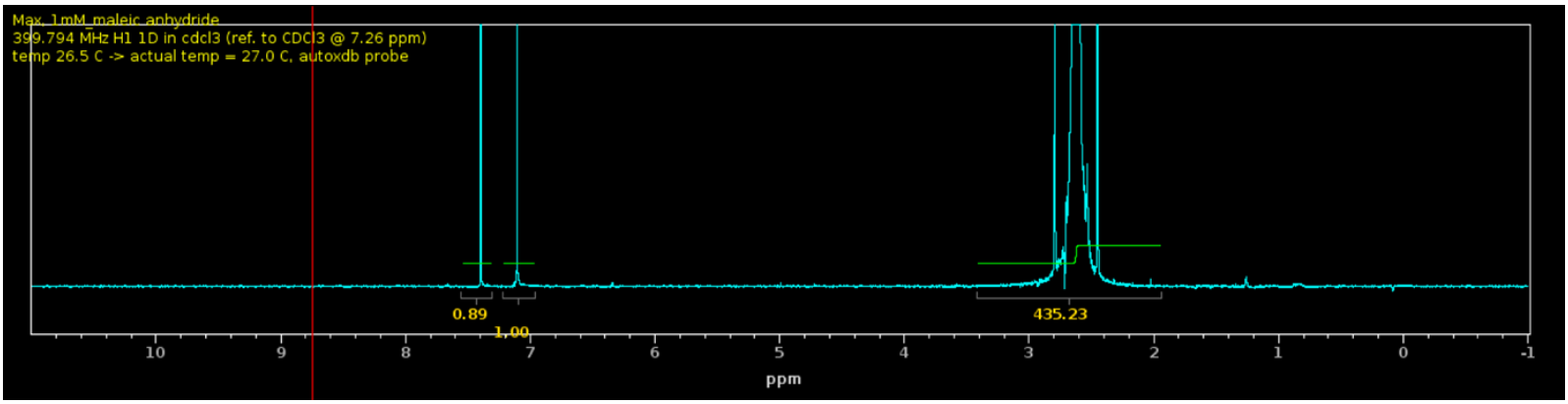


Figure S.I.1: $^1$H NMR plot of Maleic Anhydride dissolved in $CDCl_3$

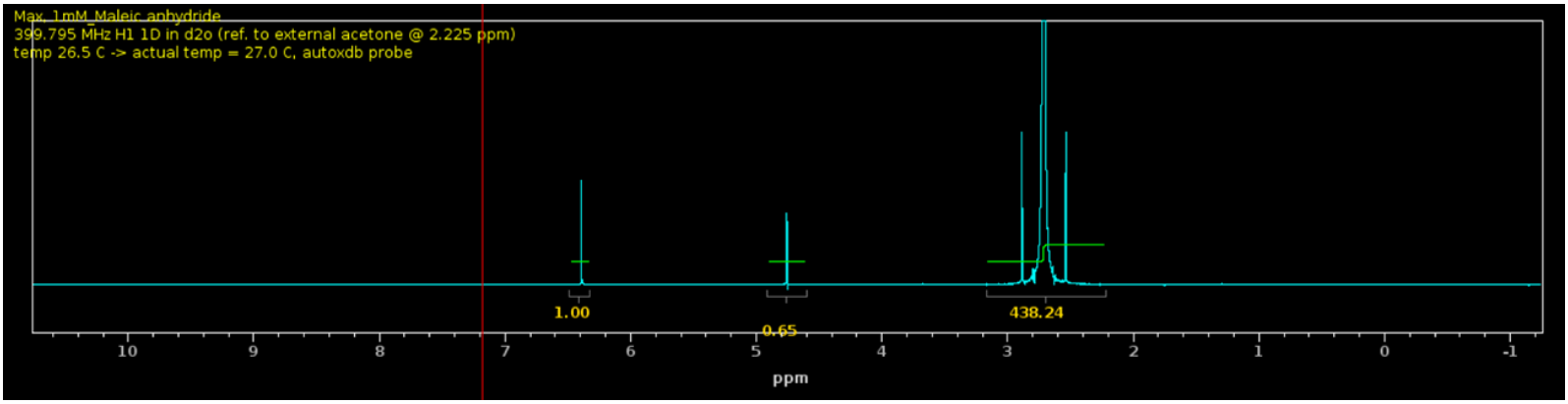


Figure S.I.2: $^{1}$H NMR plot of Maleic Anhydride dissolved in $D_2O$

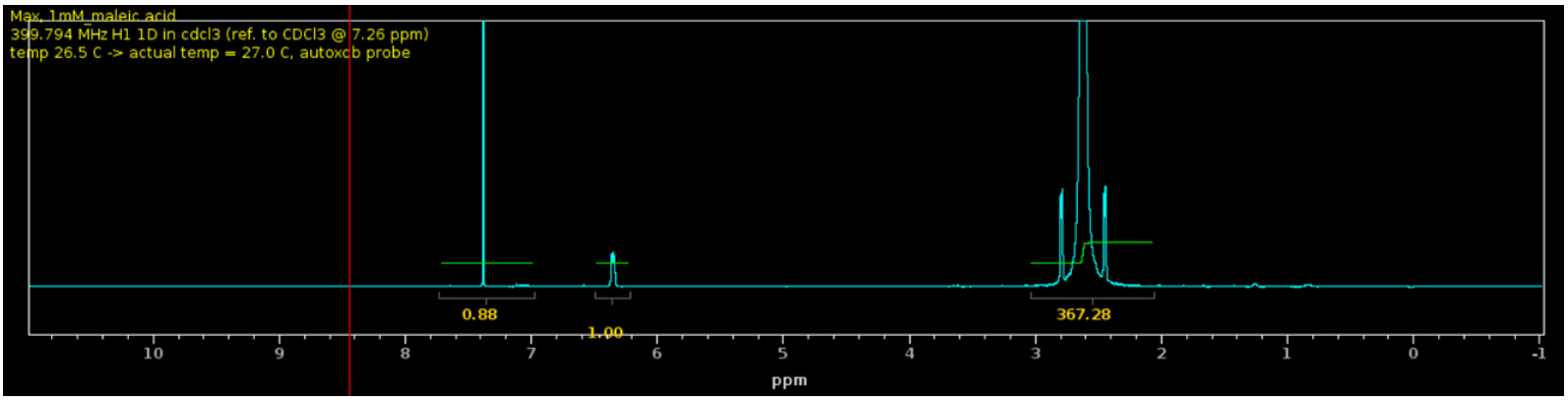


Figure S.I.3: $^{1}$H NMR plot of Maleic Acid dissolved in $CDCl_3$

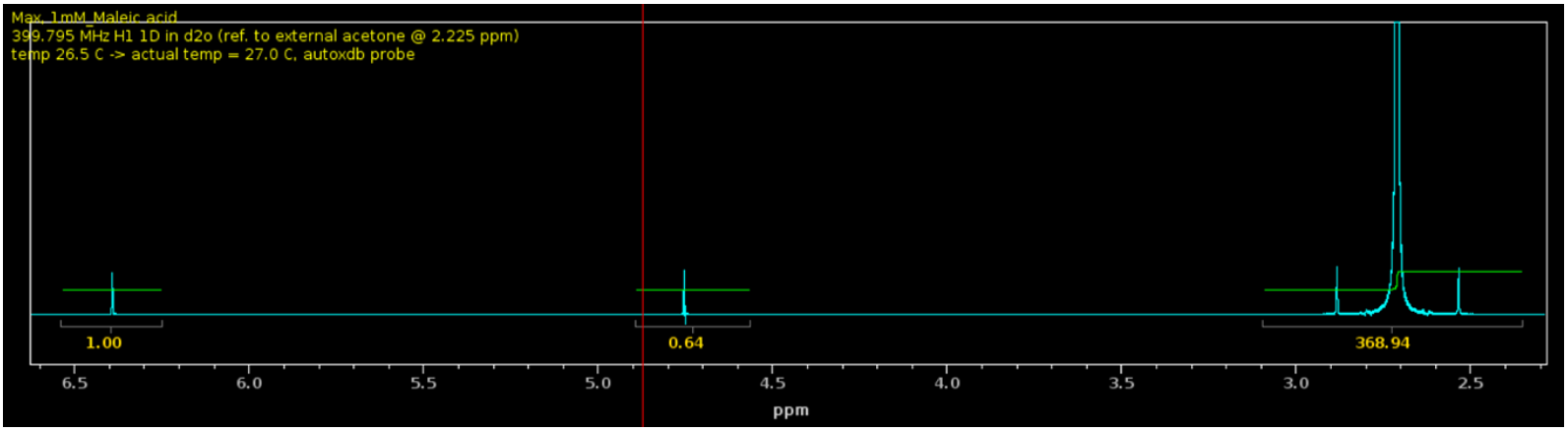


Figure S.I.4: $^{1}$H NMR plot of Maleic Acid dissolved in $D_2O$

## Section S.I.2 Anhydride Gas-Phase Concentration Determination

The gas-phase concentration of each anhydride was estimated using LC-MS and GC-FID. By flowing 200 sccm of dry air through the anhydride containing cell followed by the GC-FID and a bubbler, anhydride molecules remain trapped in the liquid water contained in the bubbler, where they rapidly hydrolyze. The water is then sampled and analyzed using the LC-MS method described in the main text. Anhydride detection is achieved through their corresponding acid peak and quantified using acid standards of known concentration. The gas-phase concentration of the anhydride flowing through the system is then back-calculated from the acid concentration in the bubbler water. The trapping efficiency of the bubbler was examined by routing the anhydride through the GC-FID after passing through the bubbler. Anhydride molecules which are not captured by the bubbler are then detected as a peak on the GC-FID. Using a similar quantity of solid anhydride as the coated tube experiments, less than 0.25% of the maleic anhydride broke-through the bubbler and was detected by the GC-FID. The breakthrough peak height did not vary significantly over a 24 h experimental period and matched background signal levels. No breakthrough peak was observed for phthalic anhydride.

## Section S.I.3 Typical LC-MS Chromatograms

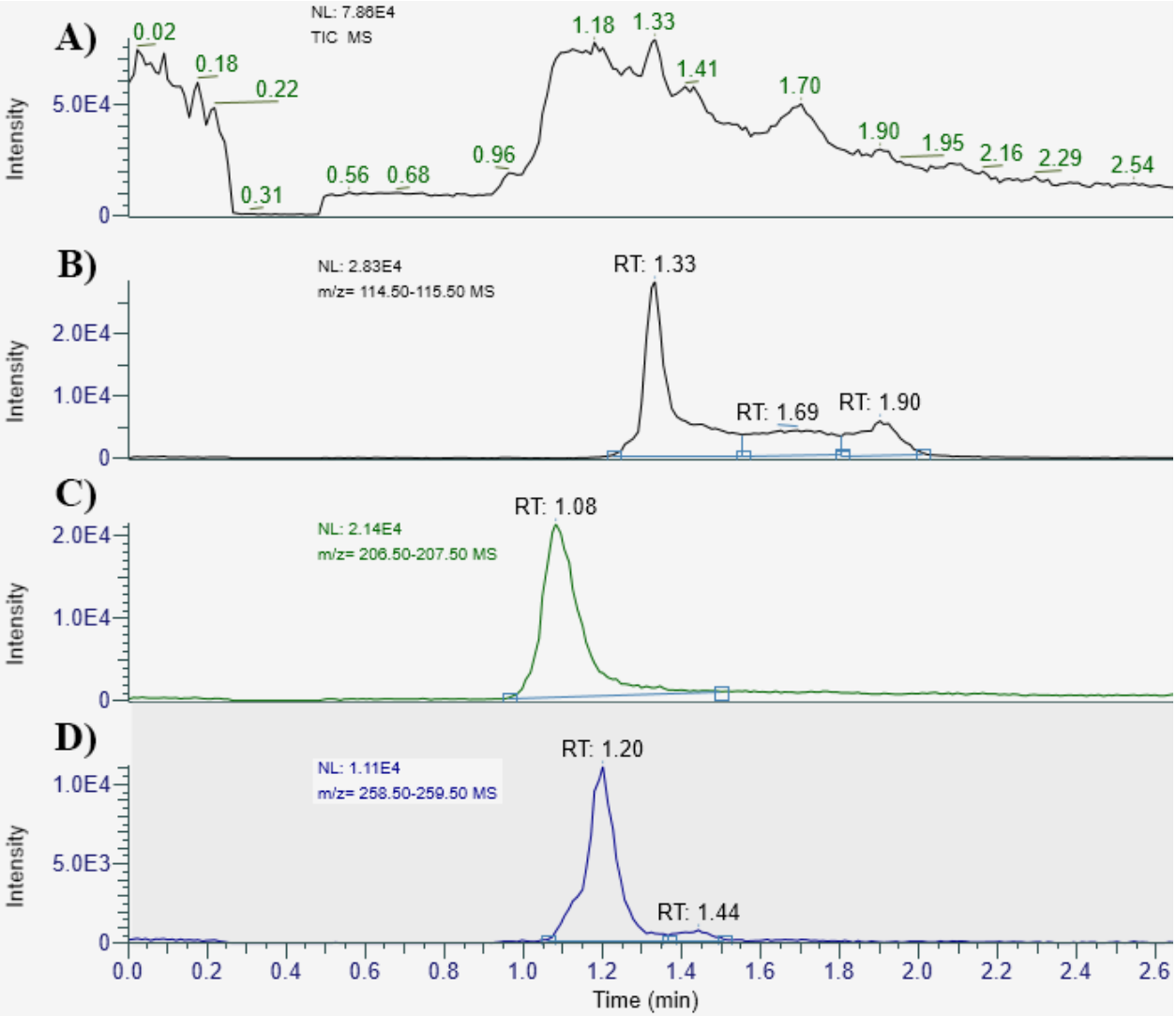


Figure S.I.5: Liquid Chromatography Negative Electrospray Ionization Mass Spectrometry (LC-MS) Plots of Coated Tube Extract After Maleic Anhydride Uptake in: (A) Total Ion Chromatogram (TIC), (B) Maleic Acid Extracted Ion Chromatogram (EIC) at a mass to charge (m/z) of 115, (C) Levoglucosan EIC at m/z 207, (D) Maleic Anhydride Levoglucosan Product EIC at m/z 259. NL represents the intensity of the largest peak in each chromatogram.

In this section, we provide typical Liquid Chromatography Mass Spectrometry (LC-MS) plots for an extracted tube (S.I.5), maleic anhydride and acid standards (S.I.7 and S.I.6), as well as phthalic acid (S.I.8) standard. As can be seen from the total ion chromatogram (TIC) in Figure S.I.5(A), a large "wave" of compounds elute at the beginning of the separa-

tion. This is usual of biomass burning emissions analyzed through LC-MS, as they contain numerous compounds with a variety of properties and functional groups.[2] (B), (C) and (D) are extracted ion chromatograms obtained from (A). As maleic anhydride does not readily ionize in negative electrospray ionization ($ESI^-$) mode, it is instead detected in its hydrolysed form as maleic acid. The peak tailing in Figure S.I.5(B) and Figure S.I.7 is typical for anhydrides samples dissolved in acetonitrile, and does not occur in the acids (Figures S.I.6 and S.I.8). Presumably, water in the LC-MS mobile phase hydrolyses the anhydride during the separation, affecting the corresponding acids retention time and peak intensity.

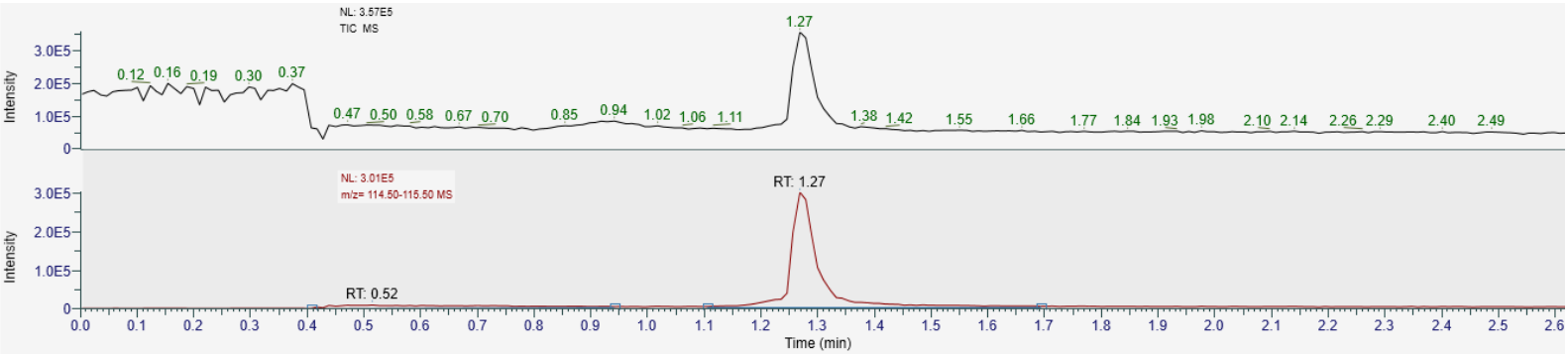


Figure S.I.6: LC-MS chromatogram of 0.01mM maleic acid dissolved in acetonitrile, TIC (top) and EIC at 115 m/z (bottom).

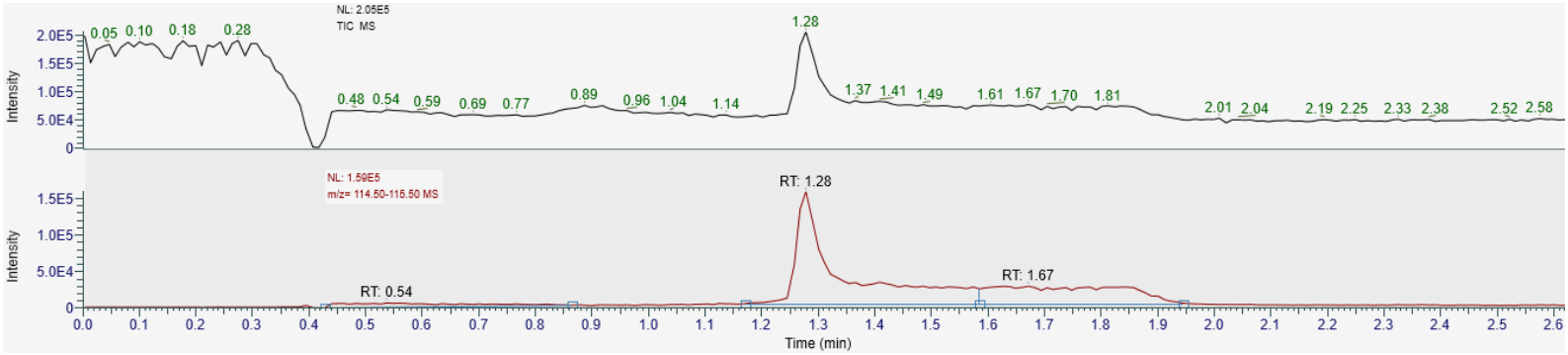


Figure S.I.7: LC-MS chromatogram of 0.1mM maleic anhydride dissolved in acetonitrile, TIC (top) and EIC at 115 m/z (bottom).

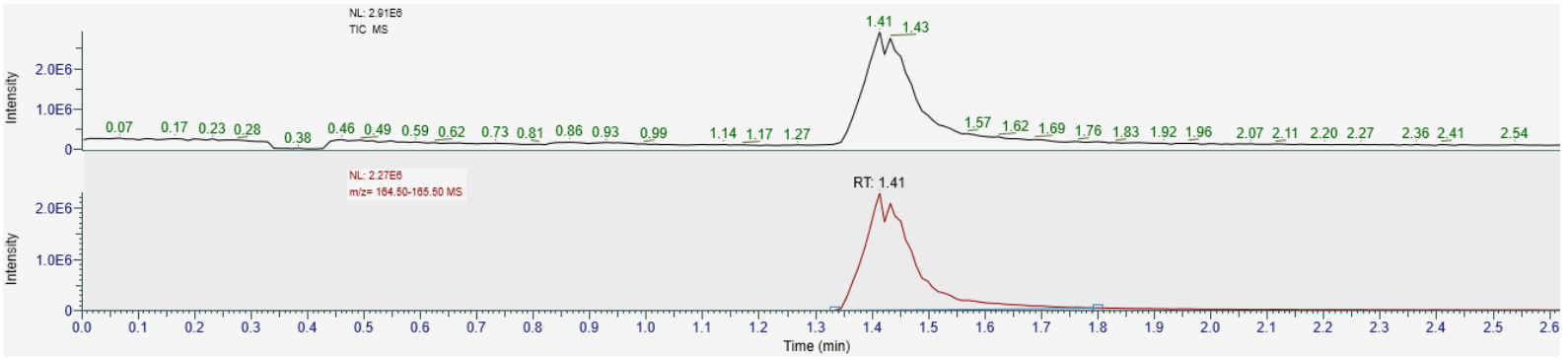


Figure S.I.8: LC-MS chromatogram of 1mM phthalic acid dissolved in acetonitrile, TIC (top) and EIC at 165 m/z (bottom).

## Section S.I.4 Burn Parameters

Table S.I.2 displays the burn and airflow parameters for each filter gathered. Emissions were gathered during the temperature ramping process and for 10 minutes after reaching 500 °C, totalling to a 14.9 min collection time. As covered in the main text, each filter was separately extracted in acetonitrile after collection, and mixed together to form a composite sample from which the tubes were coated. Assuming complete extraction, the final concentration of the composite sample was 0.00176 g/ml.

Table S.I.2: Individual filter burn parameters.

| **Sample** | **Temp (°C)** | **Flow Rate (SLPM)** | **Ext Vol (mL)** | **Sample Weight (g)** | **Filter Loading (g)** |
|---|---|---|---|---|---|
| Wood | 500 | 0.2 | 10 | 0.7162 | 0.0238 |
| Wood | 500 | 0.2 | 20 | 1.0905 | 0.0345 |
| Wood | 500 | 0.2 | 20 | 0.8827 | 0.0199 |
| Wood | 500 | 0.2 | 20 | 2.0464 | 0.0450 |
| Total | | | 70 | 4.7358 | 0.1232 |

## Section S.I.5 Coated Tube Uptake Parameters

Table S.I.3: Parameters used to calculate the uptake coefficient ($\gamma$) in Sections 2.7 and 3.2.

| Parameter | Experimental | Equation |
|---|---|---|
| Temperature (T) | 296.15 K | |
| Air Density ($\rho$) | 1.192 kg $m^{-3}$ | |
| Air Viscosity ($\eta$) | 0.0183 mPA s | |
| Coated Tube Length (L) | 20.0 cm | |
| Coated Tube Internal Diameter ($D_{tube}$) | 0.950 cm | |
| Volumetric Flow (F) | 0.204 L $min^{-1}$ | |
| Linear Velocity (v) | 4.80 cm $s^{-1}$ | $v = \frac{F}{A}$ |
| Residence Time (t) | 4.2 s | $t = \frac{v}{L}$ |
| Reynolds Number (Re)[3] | 29.7 | $Re = \frac{\rho \times D_{tube} \times v}{\eta}$ |
| Length to Laminar Flow (l)[4] | 0.989 cm | $l = 0.035 \times Re \times D_{tube}$ |
| Molecular Velocity ($\omega_x$)[5] | 205.8 m $s^{-1}$ | $\omega_x = \sqrt{\frac{8 \times k \times T}{\pi \times m}}$ |
| Air Dimensionless Diffusion Volume ($V_{Air}$)[5] | 19.7 | |
| PA Dimensionless Diff Vol ($V_{phthal}$)[5] | 136.5 | $V = \sum n_i V_i$<br>$8 \times 15.9 + 4 \times 2.31 + 3 \times 6.11$ - 18.3 |
| RM of the PA($m_A$)-Air($m_B$) Pair (m(A,B))[5] | 48.45 | $m(A,B) = \frac{2}{\frac{1}{m_A} + \frac{1}{m_B}}$ $m_A = 148.1$ $m_B = 28.96$ |
| PA Diff Coefficient (D(A,B))[5] | 0.071 $cm^2$ $s^{-2}$ | $D(A,B) = \frac{1.0868 \times T^{1.75}}{\sqrt{m(A,B)} \times (\sqrt[3]{V_{phthal}} + \sqrt[3]{V_{air}})^2 \times 760}$ |
| Mean Free Path ($\lambda$)[4] | 102.8 nm | $\lambda = \frac{D}{\omega_x}$ |
| Knudsen Number (Knx)[6] | $2.16 \times 10^{-5}$ | $Knx = \frac{2 \times \lambda}{Dtube}$ |
| Dimensionless Axial Distance ($z^*$)[4] | 0.651 | $z^* = L\frac{\pi \times D}{2F}$ |
| Effective Sherwood Number ($N_{Shw}^{eff}$)[4] | 3.80 | $N_{Shw}^{eff} = 3.6568 + \frac{A}{z^* + B}$<br>A = 0.0978 and B = 0.0154 |

PA = Phthalic Anhydride, RM = Molecular Reduced Mass

## Section S.I.6 Anhydride Nucleophilic Addition

Figure S.I.9 displays the structures predicted from the LC-MS analysis of anhydride nucleophile mixtures. In each case, the m/z of the product peak was detected as the addition of the anhydride to the nucleophile. For example, vanillin (m/z 152) and maleic anhydride (m/z 98), reacted to form a product with a m/z of 250 (detected as 249 in $ESI^-$ mode). Maleic and phthalic anhydride are used interchangeably as - with the exception of coniferyl aldehyde - both were observed to react with the listed nucleophiles.

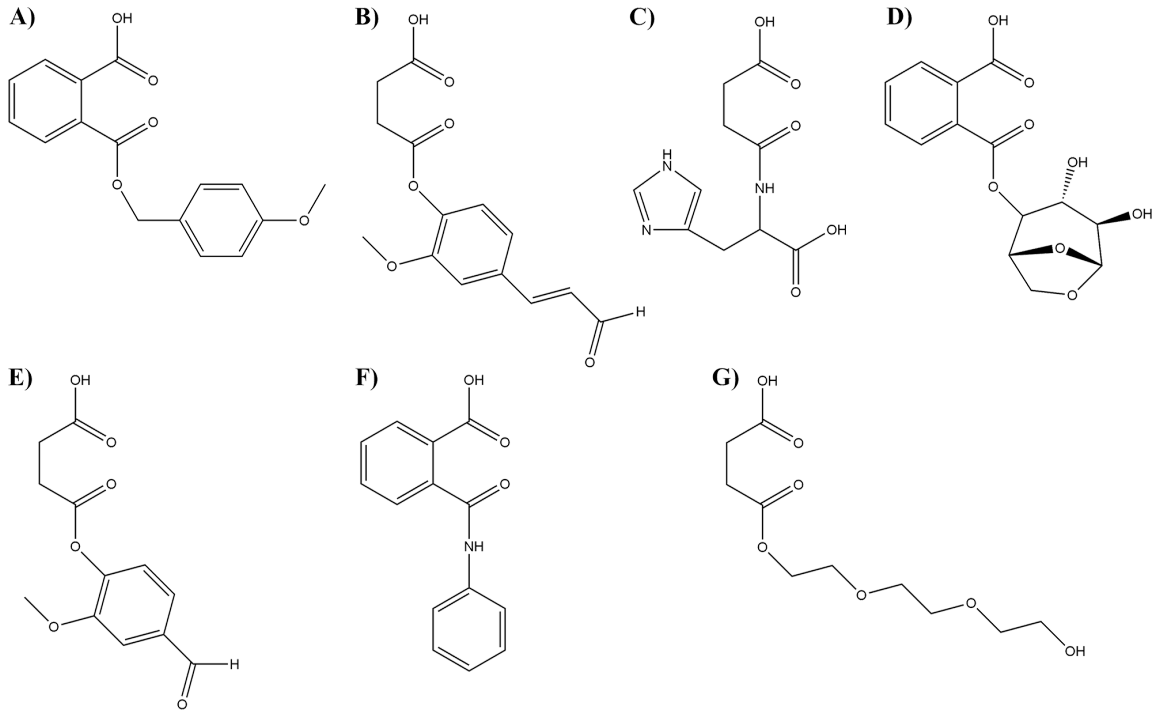


Figure S.I.9: Predicted product structures of the nucleophilic addition of anhydrides where: A) Anisyl Alcohol + Phthalic Anhydride, B) Coniferyl Aldehyde + Maleic Anhydride, C) Histidine + Maleic Anhydride, D) Levoglcusoan + Phthalic Anhydride, E) Vanillin + Maleic Anhydride, F) Aniline + Phthalic Anhydride, and G) Triethylene Glycol + Maleic Anhydride.

## Section S.I.7 Reaction Competition and Product Stability in Water

As can be seen in Figure S.I.10, the products follow similar trends as those in the main text. For MLP (B), PAP (C), and MAP (D), the presence of water (1-25%) initially enhances the formation of the product. However, the signal swiftly decays as the fraction of available water is increased. As described in the main text, it is likely that water is acting as a proton carrier during the nucleophilic addition reaction, which kick-starts the formation of the product at low water contents. As more water is made available, the hydrolysis reaction takes over and the product is formed in lower quantities.

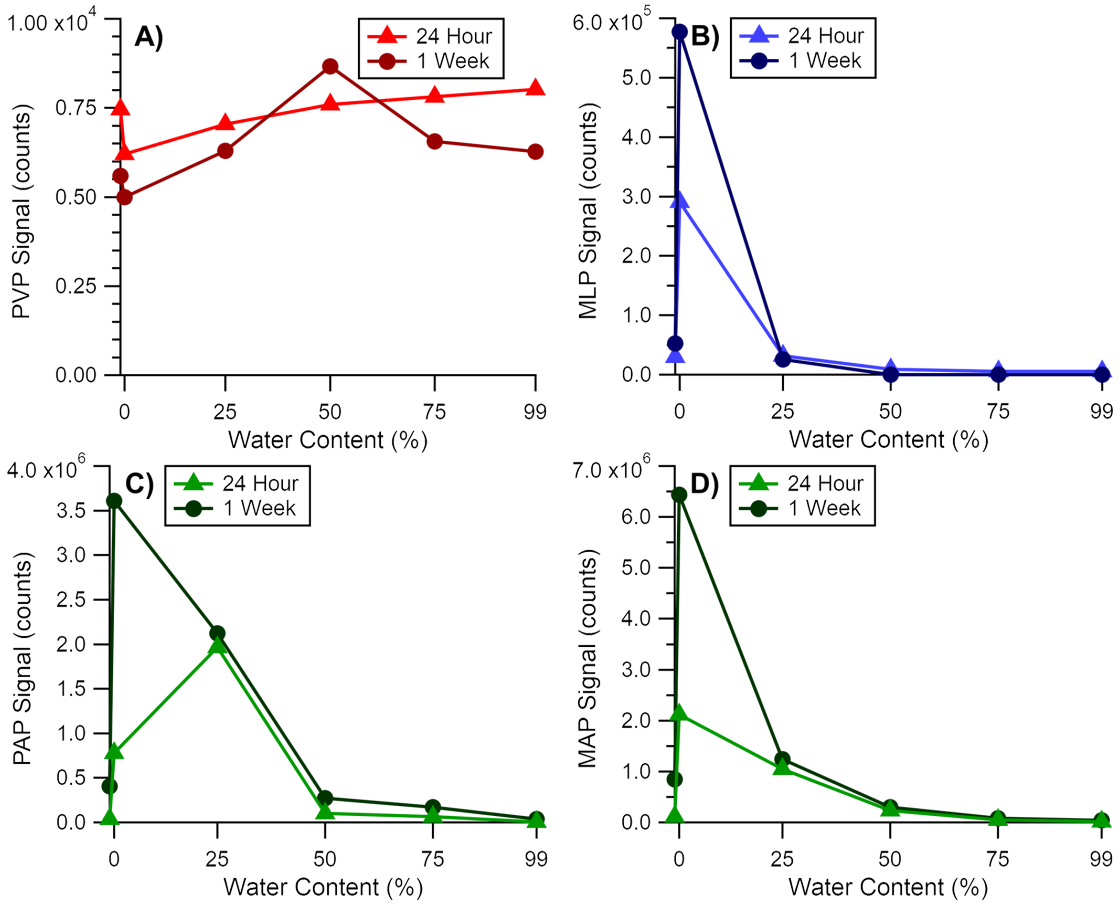


Figure S.I.10: LC-MS peak area signals obtained from increasing fractions of water in acetonitrile after the 24 hour and 1 week-long analysis period for A) Phthalic Anhydride Vanillin Product (PVP), B) Maleic Anhydride Levoglucosan Product (MLP), C) Phthalic Anhydride Anisyl Alcohol Product (PAP), D) Maleic Anhydride Anisyl Alcohol Product (MAP).

# References


(1) Gottlieb, H. E.; Kotlyar, V.; Nudelman, A. NMR Chemical Shifts of Common Laboratory Solvents as Trace Impurities. The Journal of Organic Chemistry **1997**, 62, 7512–7515, PMID: 11671879.

(2) Loebel Roson, M.; Duruisseau-Kuntz, R.; Wang, M.; Klimchuk, K.; Abel, R. J.; Harynuk, J. J.; Zhao, R. Chemical Characterization of Emissions Arising from Solid Fuel Combustion—Contrasting Wood and Cow Dung Burning. ACS Earth and Space Chemistry **2021**, 5, 2925–2937.

(3) Jennings, S. The mean free path in air. Journal of Aerosol Science **1988**, 19, 159–166.

(4) Knopf, D. A.; Pöschl, U.; Shiraiwa, M. Radial Diffusion and Penetration of Gas Molecules and Aerosol Particles through Laminar Flow Reactors, Denuders, and Sampling Tubes. Analytical Chemistry **2015**, 87, 3746–3754, PMID: 25744622.

(5) Tang, M. J.; Shiraiwa, M.; Pöschl, U.; Cox, R. A.; Kalberer, M. Compilation and evaluation of gas phase diffusion coefficients of reactive trace gases in the atmosphere: Volume 2. Diffusivities of organic compounds, pressure-normalised mean free paths, and average Knudsen numbers for gas uptake calculations. Atmospheric Chemistry and Physics **2015**, 15, 5585–5598.

(6) Pöschl, U.; Rudich, Y.; Ammann, M. Kinetic model framework for aerosol and cloud surface chemistry and gas-particle interactions — Part 1: General equations, parameters, and terminology. Atmospheric Chemistry and Physics **2007**, 7, 5989–6023.